NeuroImage 59 (2012) 2733–2742

Contents lists available at SciVerse ScienceDirect

NeuroImage

journal homepage: www.elsevier.com/locate/ynimg

Sleep spindle-related reactivation of category-specific cortical regions after learning face-scene associations

Til O. Bergmann [a,b,*], Matthias Mölle [c], Jens Diedrichs [a], Jan Born [c,d], Hartwig R. Siebner [a,e,f]

[a] Department of Neurology, Christian-Albrechts University of Kiel, Arnold-Heller-Straße 3, Haus 41, D-24105 Kiel, Germany
[b] Donders Institute for Brain, Cognition and Behaviour, Radboud University Nijmegen, NL-6500 HB Nijmegen, The Netherlands
[c] Department of Neuroendocrinology, University of Lübeck, Ratzeburger Allee 160, Haus 50, D-23538 Lübeck, Germany
[d] Institute of Medical Psychology and Behavioral Neurobiology, University of Tübingen, Germany
[e] Danish Research Center for Magnetic Resonance, Copenhagen University Hospital Hvidovre, Kettegaard Allé 30, DK-2650 Hvidovre, Denmark
[f] Institute of Neurology, Psychiatry and Senses, University of Copenhagen, Blegdamsvej 3B, DK-2200 Copenhagen, Denmark

ARTICLE INFO

Article history:
Received 28 July 2011
Revised 8 October 2011
Accepted 11 October 2011
Available online 20 October 2011

Keywords:
EEG-fMRI
Fusiform face area (FFA)
Parahippocampal place area (PPA)
Hippocampus
Paired associate learning

ABSTRACT

Newly acquired declarative memory traces are believed to be reactivated during NonREM sleep to promote their hippocampo-neocortical transfer for long-term storage. Yet it remains a major challenge to unravel the underlying neuronal mechanisms. Using simultaneous electroencephalography (EEG) and functional magnetic resonance imaging (fMRI) recordings in humans, we show that sleep spindles play a key role in the reactivation of memory-related neocortical representations. On separate days, participants either learned face-scene associations or performed a visuomotor control task. Spindle-coupled reactivation of brain regions representing the specific task stimuli was traced during subsequent NonREM sleep with EEG-informed fMRI. Relative to the control task, learning face-scene associations triggered a stronger combined activation of neocortical and hippocampal regions during subsequent sleep. Notably, reactivation did not only occur in temporal synchrony with spindle events but was tuned by ongoing variations in spindle amplitude. These learning-related increases in spindle-coupled neocortical activity were topographically specific because reactivation was restricted to the face- and scene-selective visual cortical areas previously activated during pre-sleep learning. Spindle-coupled hippocampal activation was stronger the better the participant had performed at prior learning. These results are in agreement with the notion that sleep spindles orchestrate the reactivation of new hippocampal–neocortical memories during sleep.

Introduction

When encoding new declarative memories, the hippocampus rapidly binds neocortical representations to integrated memory traces (Eichenbaum, 2000). During subsequent offline periods initially labile traces are conjointly reactivated in hippocampus and neocortex to promote the formation of hippocampus-independent cortico-cortical connections for long-term storage (Buzsaki, 1996; Frankland and Bontempi, 2005; McClelland et al., 1995, Rasch and Born, 2007). This hippocampo-neocortical reactivation preferentially occurs during non-rapid eye movement (NonREM) sleep which is well known to benefit memory consolidation from numerous behavioral and neurophysiological studies (Diekelmann and Born, 2010; Maquet, 2001; Stickgold, 2005). Yet it remains a major challenge to unravel the neuronal processes that actually mediate sleep-dependent memory consolidation.

One candidate mechanism for orchestrating neuronal plasticity in the hippocampal–neocortical circuitry is the sleep spindle (Sejnowski and Destexhe, 2000; Steriade and Timofeev, 2003), a transient oscillatory pattern of 12–16 Hz with waxing and waning amplitude that is generated in the thalamo-cortical system. Synchronized by the neocortical slow oscillation (< 1 Hz; SO) (Achermann and Borbely, 1997; Steriade et al., 1993) spindles typically coincide with sharp wave-ripples (> 100 Hz) which accompany memory trace reactivation in the hippocampus (Clemens et al., 2007; Mölle et al., 2002, 2006; Sirota et al., 2003; Steriade, 2006; Sutherland and McNaughton, 2000; Wierzynski et al., 2009). It has been proposed that the phase-locking of hippocampal ripples to single spindle cycles (Clemens et al., 2010) provides a temporal frame during which reactivated memory information is fed from the hippocampus into selected neocortical circuits (Diekelmann and Born, 2010; Mölle and Born, 2009; Siapas and Wilson, 1998; Sirota et al., 2003; Wierzynski et al., 2009). Indeed, learning-related increases in spindle number and amplitude have been observed in the human EEG (Clemens et al., 2005; Eschenko et al., 2006; Fogel and Smith, 2006; Gais et al., 2002; Schabus et al., 2004). In line with recent animal data suggesting elevated replay during periods of increased spindle activity (Johnson

* Corresponding author at: Centre for Cognitive Neuroimaging, Donders Institute for Brain, Cognition and Behaviour, Radboud University Nijmegen, P.O. Box 9101, 6500 HB Nijmegen, The Netherlands. Fax: +31 24 36 10989.
E-mail address: t.bergmann@donders.ru.nl (T.O. Bergmann).

1053-8119/$ – see front matter © 2011 Elsevier Inc. All rights reserved.
doi:10.1016/j.neuroimage.2011.10.036

et al., 2010; Peyrache et al., 2009) this study was designed to provide neuroimaging evidence for a direct involvement of sleep spindles in the reactivation of newly acquired hippocampal–neocortical memory traces in the human brain.

To tackle this issue, we performed simultaneous EEG and fMRI recordings during NonREM sleep in healthy humans. This enabled us to trace spindle-related changes in blood oxygenation level dependent (BOLD) signal (indexing regional neural activity) at high temporospatial resolution concurrently in both hippocampal and neocortical networks (Andrade et al., 2011; Dang-Vu et al., 2008; Schabus et al., 2007). EEG-informed fMRI analysis took advantage of the natural variability in spindle amplitude, modeling not only the occurrence but also the corresponding amplitude of each spindle-event. This single-trial EEG-fMRI approach (Debener et al., 2006) enabled us to identify brain regions coupled eminently to the spontaneous expression of thalamo-cortical sleep spindles. We focused on the fast centroparietal spindles which have a more pronounced spectral peak and are more likely associated with hippocampal activity as opposed to slow frontal spindles (Andrade et al., 2011; Clemens et al., 2010; Schabus et al., 2007). To test our hypothesis that the reactivation of newly encoded hippocampal–neocortical memory traces is embedded in discrete spindle events, subjects learned paired face-scene associates (Fig. 1A) or performed a non-learning visuomotor control task (Fig. 1B) on separate days before sleeping in the MRI scanner. The encoded memory traces were therefore expected to be highly specific, comprising the well-localizable face- and scene-selective regions of the ventral visual cortex (i.e., fusiform/occipital face area, FFA/OFA (Gauthier et al., 2000; Kanwisher et al., 1997) and parahippocampal place area, PPA) (Epstein and Kanwisher, 1998), as well as the hippocampus binding together these neocortical representations (Eichenbaum, 2000).

Material and methods

Participants

Twenty-four healthy volunteers participated after giving written informed consent. Participants were right-handed, free of medication, and had no history of neurological or psychiatric disease. They were not allowed to drink alcohol or caffeine during the day preceding the experiment and had to restrict their sleep to 4 h during the preceding night to increase sleep pressure. Experimental procedures conformed to the Declaration of Helsinki and were approved by the Ethics Committee of the University of Kiel. Fifteen subjects fell asleep under continuous EEG-fMRI recording in the adaptation night. Data was successfully acquired in nine subjects reaching SWS in both experimental nights (mean age: 25, range: 21–27 years, 4 female).

Experimental design and procedures

Participants took part in two experimental conditions (learning vs. control) balanced in order and separated by at least one week.

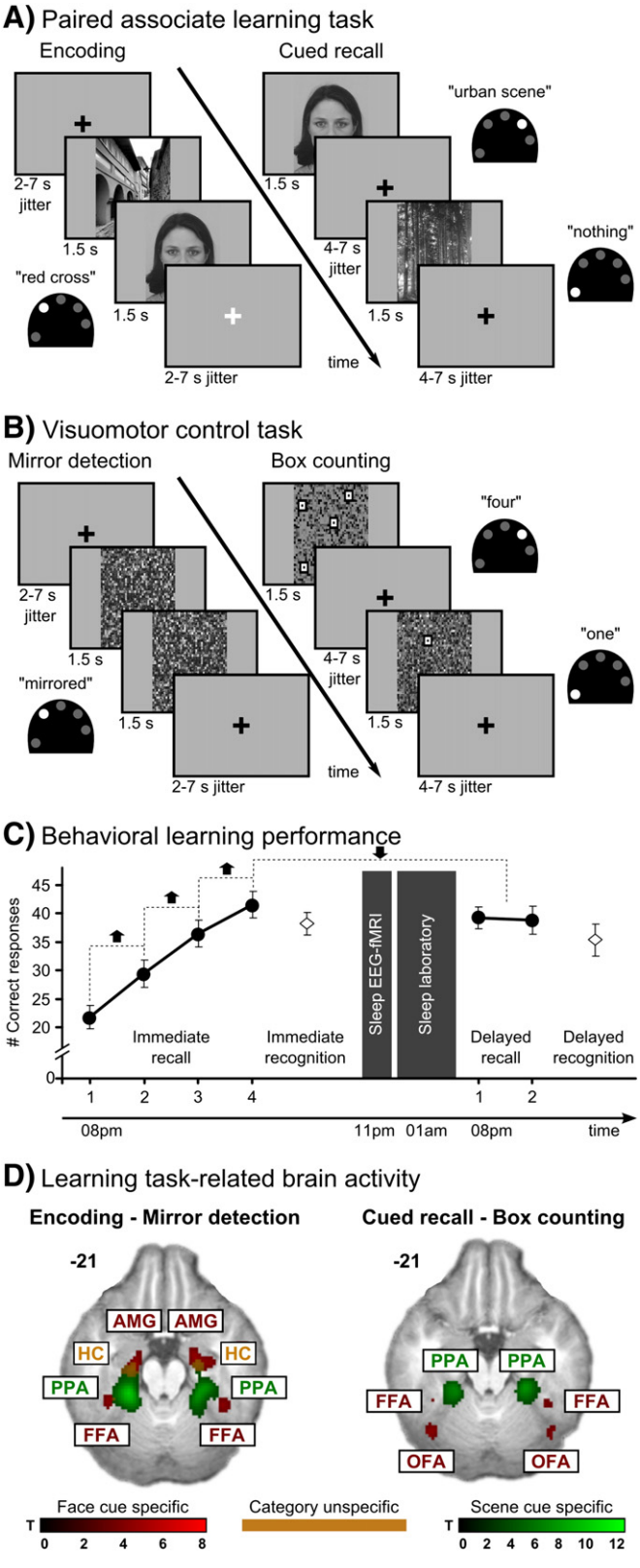

Fig. 1. Task procedures and results. (A) Paired associate learning consisted of alternating encoding and immediate cued recall runs (four of each). Encoding: subjects learned sequentially presented picture pairs and should press a button whenever the black fixation cross turned red to preserve attention. Cued recall: pictures were presented in isolation and subjects had to indicate the category of the missing associate by button press. (B) Visuomotor control task with alternating 'box counting' and 'mirror detection' runs (four of each), using the same but scrambled stimuli and identical timing. Mirror detection: subjects monitored pairs of scrambled pictures and should press a button whenever the second was a mirror image of the first to preserve attention. Box counting: subjects saw scrambled pictures and had to indicate the number of superimposed box icons by button press. See Methods and Supplementary Methods for details. (C) Behavioral performance during paired associate learning as number of correct responses (mean ± SEM) for cued recall runs (black circles) and recognition task (white diamonds) before sleep and the next evening. Arrows indicate significant changes (see Supplementary Table S2). (D) Learning task-related brain activations relative to the respective control tasks (learning > control). Color coding: Red = face cue specific, Green = scene cue specific, Orange (overlap) = category unspecific. AMG = amygdala, FFA = fusiform face area, HC = hippocampus, OFA = occipital PPA = parahippocampal place area. Functional clusters depicted on group averaged anatomical image (at MNI coordinate y = 44). Voxels are thresholded at $P_{unc} < 0.001$. Further learning task-related activations are provided in Supplementary Fig. S4.

Procedures were identical in both conditions except for the behavioral task (Fig. 1). Subjects arrived around 7 pm and performed a thorough training of the upcoming task to learn the assignment of response keys and stimulus categories until no errors were made anymore within 20 consecutive trials. Around 8 pm they completed the *Stanford Sleepiness Scale* (Hoddes et al., 1973) and started the respective task-fMRI session (lasting ~70 min). In the learning condition it was followed by a recognition task outside the scanner (Supplementary Fig. S1). After mounting the EEG cap subjects returned to the scanner around 11 pm to sleep for max. 2.5 h during continuous EEG-fMRI recordings. Subjects wore light sleeping clothes and earplugs (~35 dB sound attenuation), were bedded comfortably on a viscoelastic mattress and covered with a light blanket. Viscoelastic foam stabilized the head inside the coil and prevented unpleasant pressure from EEG electrodes. Lights were dimmed and subjects were equipped with an alarm bell to quit the experiment at any time. After awakening, subjects spent the remaining night in the adjacent sleep laboratory. They left the next morning and returned again in the evening around 8 pm for delayed cued recall (two fMRI recall or corresponding control runs) and recognition testing (outside the scanner in the learning condition).

Behavioral tasks

The paired associate learning task consisted of four runs of memory encoding, each followed by an immediate cued recall (Fig. 1A). During encoding, subjects learned 28 gray scaled picture pairs (combinations of *male faces*, *female faces*, *urban scenes*, *rural scenes*, and '*nothing*', i.e., scrambled images) which were presented on a light gray background and in pseudorandomized order. Paired pictures were presented in direct succession (1.5 s per picture) with a jittered inter-pair interval of 2–7 s (black fixation cross) and all pairs were also presented in reversed within-pair order, making up a total of 56 learning trials plus eight trials with scrambled pairs only and eight null events (fixation cross only). Subjects were asked to remember the pairs as accurately as possible by visually imagining the two pictures together (neglecting within-pair order and considering pictures paired with a scrambled image as unpaired). It was emphasized that the exact stimulus combinations instead of mere categories should be learned as they would be tested later (recognition task). Further, subjects had to press a button whenever the fixation cross briefly turned red (9 times per run) to foster sustained attention. During recall, all face and scene stimuli (48 in total) were presented in isolation (1.5 s each, inter-stimulus interval 4–7 s) and subjects were asked to retrieve the missing associate as clearly as possible and to indicate its category by pressing the corresponding of five buttons. Accuracy was strongly emphasized over speed and subjects should also respond when they could only guess. Eight pauses of 15.5 s (fixation cross) were intermingled between trials. Total run time was 9.3 min for encoding and 8 min for recall runs, resulting in a total scan time of 69.3 min.

The visuomotor control tasks were constructed in parallel (with identical timing) employing two alternating types of simple monitoring tasks, i.e., 'mirror detection' (cf. encoding) and 'box counting' (cf. cued recall). Control tasks were matched for basic visual input and motor output (the same but scrambled stimuli were presented with identical order and timing and responses with the same fingers were made at the same time) and required a certain level of attention and stimulus processing but no associative learning and no face- or scene-processing (Fig. 1B). During 'mirror detection', pairs of scrambled pictures were presented and subjects had to press a button whenever the second was a horizontal mirror image of the first (9 times per run). During 'box counting', one to five high-contrast box icons were presented on top of the scrambled images and subjects had to indicate their number by pressing one out of five buttons. No feedback of response accuracy was provided in any of the tasks.

In the recognition task subjects had to identify for each stimulus the corresponding paired associate from the complete picture set (Supplementary Fig. S1). See Supplementary Methods for a description of the stimulus material.

EEG data acquisition

32-channel EEG was acquired via MR-compatible Ag–AgCl ring electrodes with 5 kΩ safety resistors from the following locations (10–20 systems): Fp1, Fpz, Fp2, F7, F3, Fz, F4, F8, FC5, FC1, FC2, FC6, C3, Cz, C4, CP5, CP1, CP2, CP6, P7, P3, Pz, P4, P8, POz, O1, Oz, O2, T7, T8, TP9, TP10; referenced to FCz; ground ~1 cm below Oz (*BrainCap MR*, EasyCap, Munich, Germany). Skin resistance was kept below 5 kΩ (plus 5 kΩ safety resistors) using *Abralyt HiCl* electrode paste (Easycap) to ensure stable EEG recordings throughout the whole night. Bipolar recordings of vertical (below and above right eye) and horizontal electrooculogram (outer canthi), electromyogram (chin), and electrocardiogram (on the backbone, ~25 cm below and above the heart) were acquired via MR-compatible Ag–AgCl cup electrodes with 10 kΩ safety resistors (EasyCap). Data were recorded using battery-driven *BrainAmp MR plus* DC and bipolar *BrainAmp ExG MR* amplifiers, respectively (BrainProducts, Munich, Germany), transmitted via fiber optic cables to a laptop outside the scanner room, analog-filtered (0.016–250 Hz), and digitized with a resolution of 0.5 μV/bit at 5 kHz synchronized to the MR scanner clock (*BrainVision Recorder V.1.10*; BrainProducts). EEG electrodes were coregistered to individual anatomical MR images using frameless stereotaxy for consistent positioning across sessions (*TMS-Navigator*; Localite, Sankt Augustin, Germany).

EEG data analyses

Online MRI gradient and ballistocardiographic artifact correction (*BrainVision RecView V.1.2*; BrainProducts) allowed online sleep monitoring. However, removal of these artifacts for subsequent analyses was performed offline by adaptive template subtraction (Allen et al., 1998, 2000) using windows of 100 volumes and 50 pulses, respectively (*BrainVision Analyzer V. 2.0*; BrainProducts). EEG data were re-referenced to linked mastoids (i.e., TP9 and TP10) and sleep stages were visually scored according to standard criteria (Rechtschaffen and Kales, 1968). Sleep spindles and slow oscillations (SOs) were then automatically detected by well-established thresholding algorithms (Gais et al., 2002; Mölle et al., 2002) using *Spike2 V. 6.0* software (CED).

We limited spindle detection and analyses to the classical "fast centroparietal" sleep spindle around 12–14 Hz which serves as a defining feature of human NonREM sleep (Rechtschaffen and Kales, 1968). Since these spindles are clearly reflected by a pronounced peak in the EEG power spectrum of every single subject, we determined individual spindle peak frequencies (13.6 ± 0.38 Hz; mean ± SD). Individual spindle band was defined as peak frequency ± 1.5 Hz instead of using the same frequency range for all subjects in order to increase the accuracy of our analysis (Supplementary Fig. S2 and Supplementary Table S1). Spindle detection was applied to all artifact-free 30-s NonREM epochs (i.e., including stage 2 and SWS) in each of the 10 centroparietal channels that expressed the largest individual spindle power (i.e., C3, Cz, C4, CP5, CP1, CP2, CP6, P3, Pz, P4 in all subjects). EEG data were bandpass filtered (peak frequency ± 1.5 Hz) and the root mean square (RMS) was calculated using a moving average window of 0.2 s. For all channels amplitude threshold was set to 0.8 times the average standard deviation of the 10 channels. The comparatively liberal amplitude criterion of 0.8 SD was deliberately chosen to gain sufficient variance for explicit modeling of spindle amplitude in the fMRI analysis. In each channel a spindle was detected only if the RMS signal remained suprathreshold for 0.5–3 s (duration criterion). Since we wished to include only the most consistent spindles, the same algorithm was applied to an average

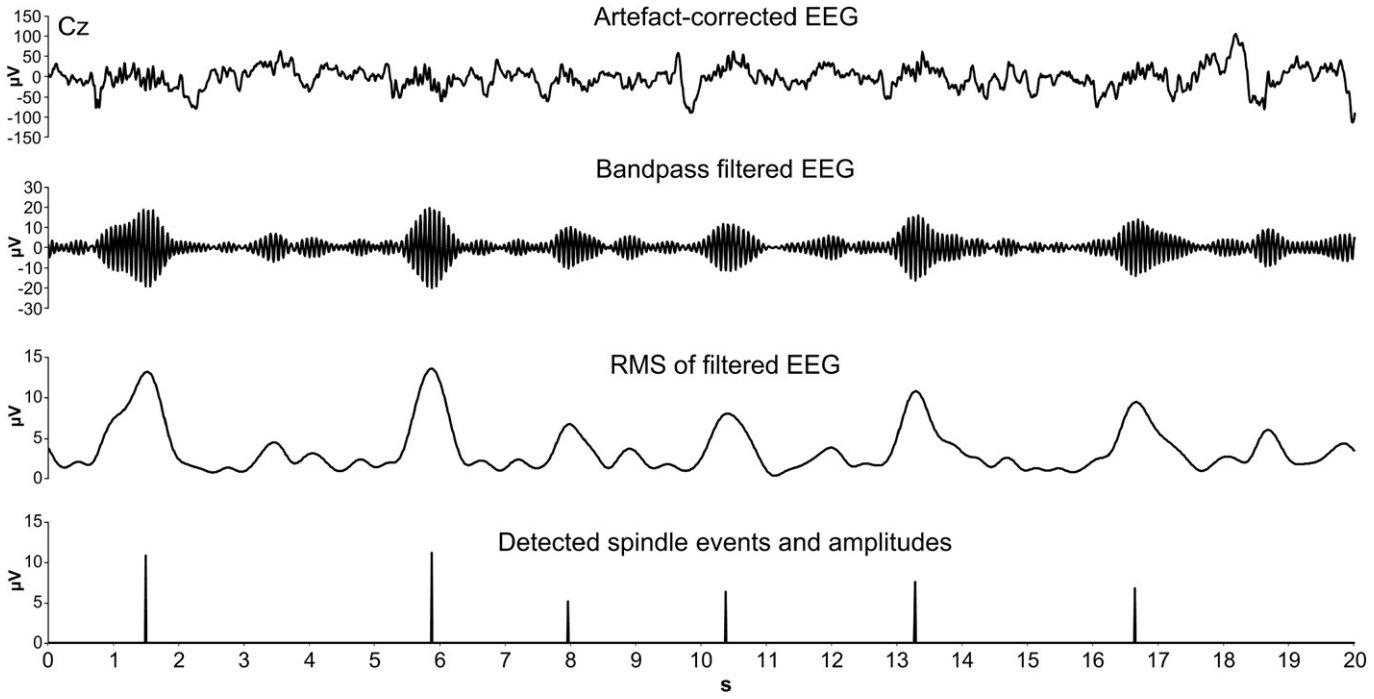

Fig. 2. Spindle detection. Example data strip of channel Cz for a single subject (a 20 s epoch was chosen to preserve visibility of the spindle signal) to illustrate the spindle detection procedure. The rows (from top to bottom) represent the artifact corrected raw EEG signal, the spindle bandpass filtered (peak frequency ± 1.5 Hz) signal, the RMS signal (smoothed by a 200 ms moving average), and the stick functions indicating detected spindle events and corresponding amplitudes from the average RMS channel used to inform the EEG-fMRI analysis. Detailed information on the spindle detection procedure and criteria are provided in the Methods section.

RMS channel (across the 10 original channels). Only when detection criteria were simultaneously met in both the average channel and in at least 5 original channels a spindle event was included in the subsequent singe-trial EEG-fMRI analysis. The peak time (deepest trough) of the largest spindle was determined from the filtered signal and represented the respective spindle in time. This temporal

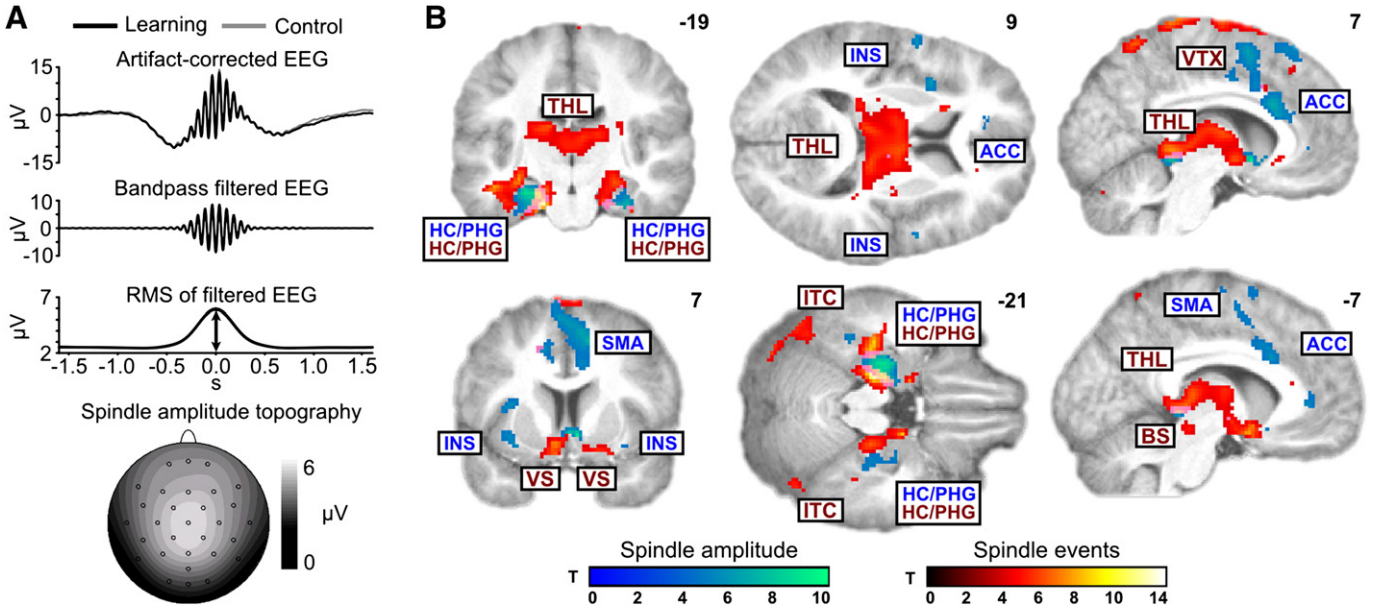

Fig. 3. General spindle effects. (A) Sleep spindle detection: waveforms depict grand averages of detected sleep spindles in the artifact-corrected, bandpass filtered, and root mean square (RMS) EEG signal both for learning (black line) and control (gray line) nights. The arrow indicates spindle amplitude as determined for single-trial EEG-fMRI analysis (Fig. S2 for an illustration of single subject data). The map depicts the topography of detected sleep spindle amplitudes with the typical centro-parietal peak. (B) Brain areas showing a positive BOLD response to the occurrence of sleep spindles independent of their amplitude (hot colors; event regressor) or a BOLD response depending in its amplitude on the corresponding spindle amplitude (cold colors; amplitude regressor). Violet shades indicate overlaps due to additive color coding. ACC = anterior cingulate cortex, BS = brainstem, HC = hippocampus, INS = Insula, ITC = Inferior temporal cortex, SMA = supplementary motor area, PHG = parahippocampal gyrus, THL = thalamus, VS = ventral striatum, VTX = vertex. Functional clusters are depicted on the group averaged anatomical image (MNI coordinate given for each slice). Voxels are thresholded at $P_{unc} < 0.001$.

information was used to define spindle events in the fMRI analysis whereas the corresponding RMS maximum from the average channel was used as an index of spindle amplitude modulation over time. The amplitude modulation was implemented in subsequent event-related fMRI analysis as an additional parametric modulator of the spindle related BOLD response (Figs. 2 and 3A). In addition, also SOs were included in the fMRI analysis (see Supplementary Methods for details on SO detection) to partial out the impact of SOs on the BOLD signal (Dang-Vu et al., 2008; Schabus et al., 2007).

fMRI data acquisition

fMRI was performed on a 3 Tesla MR scanner (*Philips Achieva*; Philips Medical Systems, Best, The Netherlands). High-resolution T1-weighted anatomical images were obtained using a standard MPRAGE sequence (TR = 7.7 ms, TE = 3.6 ms, flip angle = 8°, 170 sagittal slices, 1 × 1 × 1 mm voxel size, field of view = 224 × 224 mm). For task-fMRI, we used an echo planar imaging (EPI) sequence (TR = 2500 ms, TE = 37 ms, flip angle = 90°, FOV = 216 × 216 mm, 38 transversal slices, slice thickness = 3 mm, gap = 10%, in plane voxel size = 3.38 × 3.38 mm, continuous bottom-up slice acquisition order). Sleep-fMRI parameters were slightly modified (TR = 2240 ms, TE = 30 ms) to ensure that residual gradient artifacts (in the slice repetition rate of ~17 Hz) did not compromise the sleep spindle frequency.

fMRI data analyses

Preprocessing

fMRI data were analyzed using *SPM5* (www.fil.ion.ucl.ac.uk/spm) running on *Matlab 7.7* (The MathWorks, Natick, MA, USA). EPI volumes were slice time corrected (with reference to the middle slice of each volume) and realigned to the mean image (4th order b-spline interpolation). Individual T1-weighted images were coregistered to the mean EPI, segmented using the tissue probability maps provided by SPM5, and concurrently transformed into the standard Montreal Neurological Institute (MNI) space. EPI volumes were then normalized with the same spatial transformation and smoothed using an 8 mm full-width at half-maximum isotropic Gaussian kernel. For topographical interpretation and illustration purposes a group averaged normalized T1-weighted image was calculated.

Task-fMRI analyses

Task-fMRI analyses mainly contrasted learning and control tasks to identify the exact location of the face- and scene-selective ventral visual cortex regions that represent the paired associate learning material relative to its scrambled versions from the control task (cf. Epstein and Kanwisher, 1998; Gauthier et al., 2000; Kanwisher et al., 1997). Separate first level (single subject, fixed-effects) models were calculated for memory encoding (four pre-sleep runs) and immediate cued recall (four pre- and two post-sleep runs) for both learning and control. Face (F), scene (S) and scrambled (N, 'noting') stimuli were modeled as follows. For encoding, nine event regressors (1st stimulus: F/S/N × 2nd stimulus: F/S/N; or the respective scrambled control trials) were modeled as 3 s epochs (duration of one pair) convolved with the canonical hemodynamic response function (HRF). For recall, six event regressors (cue: F/S × target: F/S/N; or the respective scrambled control trials) were modeled as stick functions convolved with the canonical HRF. Either five (encoding: F–F, S–S, F–S/S–F, F–N/N–F, S–N/N–S) or six (recall: F–F, F–S, F–N, S–F, S–S, S–N) contrast images (plus the same number for the matched control trials) pooled across the respective runs were defined as input for the group analyses.

On the second level (group, random-effects), to determine the learning-specific brain regions during pre-sleep wakefulness, two separate flexible factorial designs were specified for encoding and recall, comprising the factors *subject* (nine subjects, independent levels, equal variance), *task* (learning vs. control, dependent levels, equal variance), and *trial type* (either five or six trial types, dependent levels, equal variance). Differential contrasts (learning > control) were calculated separately for face and scene trials to highlight the respective category-specific brain regions. To investigate overnight changes in recall-related activation, another model was set up in parallel which contrasted the last pre-sleep recall run with the post-sleep recall session. In addition, a regression model was specified, predicting the overnight change in recall-related activation based on the

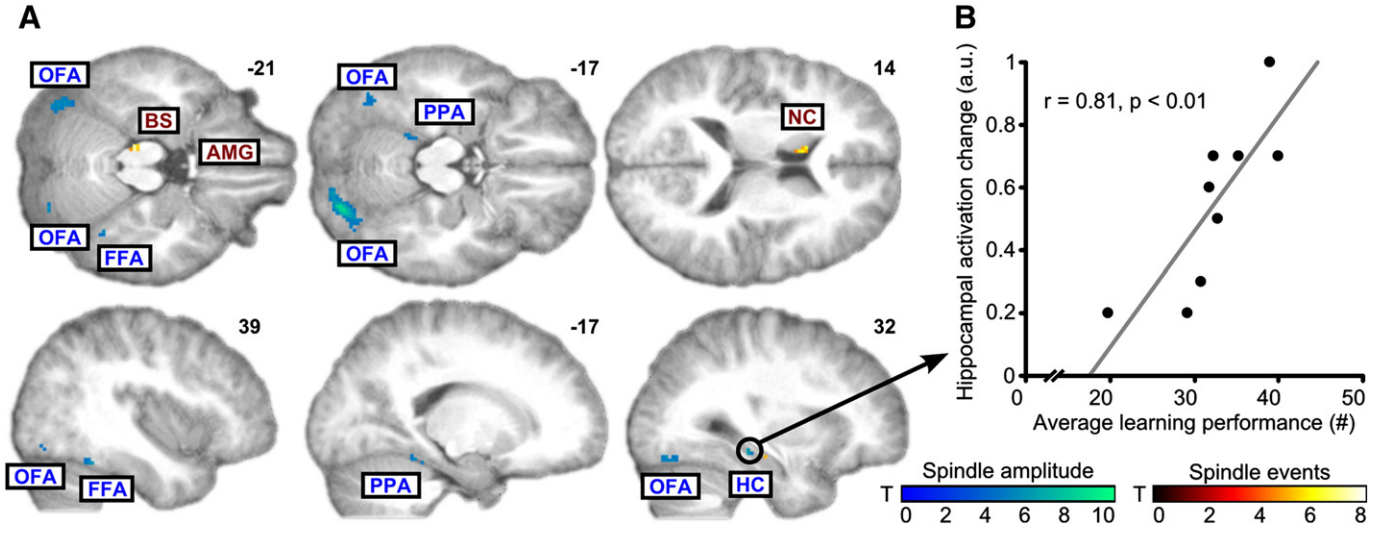

Fig. 4. Learning-dependent spindle effects (learning > control). (A) Brain areas showing learning-specific increases in coupling to spindle amplitude (cold colors) relative to the control condition (hot colors indicate amplitude-independent increases for spindle events; Supplementary Table S9). AMG = amygdala (not visible in the selected slice), BS = brainstem, FFA = fusiform face area, HC = hippocampus, NC = Caudate nucleus, OFA = occipital face area, PPA = parahippocampal place area. Functional clusters are depicted on the group averaged anatomical image (MNI coordinate given for each slice). All depicted voxels are significant at $P_{unc} < 0.001$ (only cluster ≥ 5 voxels are labeled). Overlap with task activity is shown in Supplementary Fig. S5 at $P_{unc} < 0.01$. (B) Correlation between the average individual learning performance (average number of correct recalls per run) and subsequent individual increase in spindle-related hippocampal activity during subsequent sleep (learning minus control; peak voxel at xyz = 32, −28, −12).

individual spindle-related hippocampal activation that was found to correlate with pre-sleep task performance (see Results and Fig. 4B).

Sleep-fMRI analyses

Sleep-fMRI analyses addressed two main aspects. First, we aimed to determine brain regions showing a change in BOLD signal with the occurrence of sleep spindles irrespective of the experimental condition (learning vs. control). We tested for both, categorical BOLD signal changes associated with the expression of sleep spindles per se and gradual BOLD signal changes depending on trial-by-trial variations in spindle amplitude. We reasoned that these brain regions comprise neurons that are particularly responsive to the thalamocortical sleep spindle. A second line of analysis tested our actual hypothesis. Here we examined whether hippocampus, FFA/OFA, and PPA showed stronger spindle-associated activation after learning than the control task in response to spindles per se and in particular a response that covaried with spindle amplitude. In each subject, continuous EPI time-series of artifact free NREM sleep (stage 2 and SWS; uninterrupted by arousals, awakenings or stage 1 sleep) were concatenated within nights and entered as separate learning and control runs into a fixed-effects analyses (SPM first level). To account for potential mean signal differences across concatenated EPI series, separate block regressors were included for each continuous EPI series after removing the default session-wise block regressors. Default high-pass filters were switched off and filters were instead modeled explicitly by regressor sets of cosine functions separately for each continuous EPI series to avoid artifacts at discontinuities between concatenated EPI series (128 s high-pass filter sets generated by the SPM5 *spm_filter.m* function).

Modeling of individual sleep spindles included an event regressor capturing the detected spindle peaks and a parametrical modulator reflecting the temporal modulation of spindle amplitudes. Respective regressors were also included for SOs and their amplitudes which were not the target of the present analyses. Modeling of the associated BOLD signal changes on the single subject level reduces the unexplained error variance in the BOLD signal and also avoids the overestimation of spindle-related signal changes due to overlapping SO-related BOLD responses (Dang-Vu et al., 2008; Schabus et al., 2007). Event and parametric regressors were convolved with the canonical HRF and with its time and dispersion derivatives. We took special care to model potentially confounding BOLD signal changes induced by head movement or cardiac cycle as nuisance regressors. Movement regressors consisted of the six realignment parameters (translations in x, y, and z directions and rotations around x, y, and z axes) and their squares both of the current and the previous volume to account for spin history effects (24 regressors in total). Effects of changes in blood flow due to the cardiac cycle were modeled by convolution of the R–R ECG interval with a 5th order set of sine and cosine functions (*RETROICOR*) (Glover et al., 2000), resulting in 10 additional regressors. To test spindle effects on the group level, learning and control parameter estimates (beta values) of spindle event and amplitude regressors were entered into random-effects analyses (SPM second level). Resulting t-maps were color-coded and superimposed on the group averaged structural MRI using *MRIcron* (www.cabiatl.com/mricro/mricron).

Statistics

Unless specified otherwise, behavioral and electrophysiological data are reported as mean ± standard deviation (SD). Statistical comparisons relied on two-sided paired t-tests with P-values <0.05 considered significant. For fMRI data, one-sided one-sample t-tests revealed general BOLD correlates of sleep spindles. One-sided paired t-tests revealed brain regions more strongly coupled to sleep spindles after learning than control. We had precise a priori predictions which areas should conjointly increase their responsiveness to sleep spindles after learning compared to control, i.e., the activations in FFA, OFA, PPA, and the hippocampus observed during prior learning. We therefore based the small volume correction (SVC; $P_{SVC}<0.05$) for multiple comparisons in the sleep dataset on a priori defined brain regions of interest that were extracted from an independent dataset, i.e., the preceding task fMRI session (learning > control) (for a critical view on SVC see Poldrack and Mumford, 2009). SVC search volumes were defined as spheres with 8 mm radius around the center-of-mass of the respective clusters (learning task > control task at $P_{unc}<0.001$; Fig. 1D): left PPA (−24, −45, −12), right PPA (25, −44, −12), left FFA (−38, −45, −23), right FFA (41, −46, −23), left OFA (−40, −66, −17), right OFA (36, −80, −12), left hippocampus (−23, −21, −21), right hippocampus (23, −15, −21). However, as tradeoff between specificity (not to neglect activation in other brain areas) and sensitivity (not to miss true activation), we always provide results from whole brain analyses (not restricted to predefined regions of interest) at a significance threshold of $P_{unc}<0.001$ (uncorrected for multiple comparisons) and a cluster extend threshold of 5 voxels (accounting for the small volume of our target regions).

Results

Paired associate learning

Data are reported from 9 out of 24 subjects who managed to reach SWS during EEG-fMRI in both experimental nights (see Methods). All of them successfully learned the paired associations with monotonic improvement across successive immediate cued recall runs (Fig. 1C; Supplementary Table S2). They recalled 87 ± 14% (mean ± SD) of the paired associates in the final run and still showed high retention rates (81 ± 14%) during delayed recall the next evening. Additional recognition testing (Supplementary Fig. S1) revealed that 80 ± 13% (74 ± 18% the next evening) of the pictures were correctly assigned to their specific associate, indicating that in fact stimulus–stimulus rather than mere stimulus–response associations were learned.

Brain activations during pre-sleep encoding and immediate recall runs relative to activations during the respective control tasks (learning > control) confirmed the expected involvement of face- and scene-selective ventral visual cortex as well as the hippocampus in learning (Fig. 1D). Face-specific activity was predominant bilaterally in FFA and OFA (recall only), and amygdala (encoding only). Scene-specific responses were most pronounced in bilateral PPA, the parieto-occipital sulcus, retrosplenial cortex, the transverse occipital and intraparietal sulci. The hippocampus was bilaterally activated during encoding of paired associates independent of learning material. See Supplementary Fig. S4 and Supplementary Tables S5–6 for further learning task-related brain regions. In addition the entire recall network was more strongly activated during post-sleep delayed recall the next evening than during the final pre-sleep recall run.

Table 1
Learning-specific increases in spindle-amplitude dependent brain activity.

Brain region	x	y	z	T	P_{unc}	P_{SVC}
Hippocampus (R)	32	−28	−12	6.14	0.000139	n.a.
FFA (R)	40	−46	−22	5.85	0.000191	0.031
PPA (L)	−18	−42	−16	5.20	0.000411	0.049
OFA (R)	24	−82	−18	9.59	0.000006	0.030
OFA (L)	−36	−74	−22	6.20	0.000130	0.043

Notes: MNI coordinates (x, y, z) and T-values are provided for the peak voxels of all clusters with an extent threshold ≥ 5 voxel and significant at $P_{unc}<0.001$ (exact P_{unc} values given for each peak). Activations with $P_{SVC}<0.05$ survived correction for multiple comparisons on small volumes of interest as defined by the previous face- and scene specific activations of the learning task (learning > control); see Methods for details. R = right, L = Left.

Spindle-coupled brain activity independent of experimental condition

Sleep spindles detected in the surface EEG to inform single-trial EEG-fMRI analyses by their corresponding amplitude showed the typical waxing and waning pattern (Fig. 3A; Supplementary Fig. S3). Independent of the experimental learning vs. control condition, the occurrence of spindle events per se (i.e., irrespective its corresponding amplitude) was associated with BOLD responses in the bilateral thalamus, hippocampus and adjacent parahippocampal gyrus, ventral striatum, brainstem, inferior temporal cortex and cortical regions around the vertex (Fig. 3B; Supplementary Table S7). Of note, the BOLD response in bilateral hippocampus was clearly modulated by spindle amplitude, i.e., the higher the spindle amplitude the stronger was the activity in these hippocampal regions. The same amplitude-dependent modulation of the BOLD signal was observed in bilateral insula, anterior cingulate cortex, supplementary motor area, ventral striatum, and a small thalamic cluster (Supplementary Table S8). Neither the occurrence nor the amplitude of sleep spindles were associated with any decrease in BOLD signal.

Learning-dependent increase in spindle-coupled brain activity

Compared to the visuomotor control task, paired associate learning before sleep increased coupling of neuronal activity to spindle amplitude in a distinct set of brain regions (learning > control; Fig. 4A). The learning-specific increase in coupling between spindle amplitude and brain activity was restricted to clusters in the left PPA, the right FFA, bilateral OFA (all $P_{SVC}<0.05$) as well as the right hippocampus ($P_{unc}<0.001$) (Table 1; see Supplementary Table S9 for additional amplitude-independent results). The location of neocortical clusters matched the face- and scene-specific activations observed during the prior learning task (overlap maps are provided in Supplementary Fig. S5). For PPA and FFA, activations were located almost entirely within the corresponding encoding and retrieval task-related clusters, and for the OFA there was a considerable overlap with previous recall task-related activations.

In the hippocampus, the increase in spindle-coupled activity was located in the middle of its longitudinal axis, slightly posterior to the hippocampal activations observed during memory encoding. Correlational analyses linked this activation to individual learning performance: the better a subject performed on the learning task (average number of correctly recalled paired associates) before sleep, the more pronounced was the learning-specific increase (relative to the control night) in coupling between spindle amplitude and hippocampal activity ($r=0.81$, $P<0.01$; Fig. 4B). The same holds true for the learning slope (average increase per run; $r=0.67$, $P<0.05$). However, the increase in spindle-related hippocampal activation did neither predict one-day retention of the learned associates (indicated by the ratio of delayed to immediate cued recall or recognition) nor the observed overnight increase in recall-related BOLD response.

Spindle-informed fMRI comparisons between sleep after learning and control sleep were not biased by general differences between the sessions. Sleep architecture was closely comparable (Supplementary Table S3) and none of the relevant parameters differed between sessions, i.e., total scan time and analyzed sleep time, number of 30-s epochs in NonREM sleep stage 2 and slow wave sleep (SWS) included in the fMRI analysis, as well as number, density and amplitude of sleep spindles and SOs (all $P>0.3$; Supplementary Table S4). Subjects also reported similar levels of sleepiness prior to task performance (Stanford Sleepiness Scale: 4.8 ± 1.2 vs. 5.2 ± 1.3; $P>0.3$).

Discussion

Prior learning of face-scene associations gave rise to a stronger coupling between sleep spindles and neural activity in face- and scene-selective regions of the ventral visual cortex as well as the hippocampus. Specifically, neural activity in these regions covaried more closely with ongoing variations in spindle amplitude after learning than after a non-learning visuomotor control task. The increase in coupling between spindle amplitude and brain activity was clearly related to previous learning. In the neocortex, increased coupling was topographically restricted to face- and scene-specific regions that were active during prior learning. In the hippocampus, increased coupling was predicted by individual learning performance before sleep. Our findings are consistent with the idea that spindles represent a key mechanism for hippocampal-neocortical reprocessing of recently acquired memory traces during sleep, although in the light of the relatively small sample size only cautious conclusions can be drawn (Diekelmann and Born, 2010; Marshall and Born, 2007; Sejnowski and Destexhe, 2000; Steriade and Timofeev, 2003).

Paired associate learning

We chose a paired associate learning task which not only relied on the hippocampus, binding together neocortical representations (Eichenbaum, 2000; Frankland and Bontempi, 2005), but also strongly engaged category-specific neocortical regions of the ventral visual cortex, i.e., FFA (Kanwisher et al., 1997), OFA (Gauthier et al., 2000), and PPA (Epstein and Kanwisher, 1998) compared to a visuomotor control task. This allowed us to identify neocortical regions as candidate areas that would show learning-specific reactivation, conjointly with the hippocampus, during subsequent sleep spindles. Although sleep deprivation or disrupted SWS can be detrimental to encoding performance and related hippocampal activity (Van Der Werf et al., 2009; Yoo et al., 2007), our subjects still showed good learning performance together with distinct encoding-related hippocampal activation, probably because the relatively mild sleep restriction in our study did not affect the SWS rich first half of the night. Importantly, sleep restriction and accompanying tiredness did not differ between experimental conditions.

Spindle-coupled brain activity independent of experimental condition

Hippocampal spindle coupling

Extending previous findings (Schabus et al., 2007), we observed task-independent spindle-related regional neuronal activity in various brain regions including – most importantly – the hippocampus. The pronounced bilateral activation of hippocampus and adjacent parahippocampal gyrus was not only associated with the mere occurrence of sleep spindles but was also modulated by spindle amplitude. The hippocampal BOLD response was greater the larger the spindle amplitude. This observation suggests a tight link between hippocampal network activity and spindle input that goes beyond a mere temporal synchrony of thalamo-cortical spindles and hippocampal sharp-wave ripple activity as revealed by intracranial recordings (Clemens et al., 2007; Mölle et al., 2009; Siapas and Wilson, 1998; Sirota et al., 2003; Wierzynski et al., 2009). Within an interactive framework of neocortical–hippocampal loops, emergent spindle activity might drive hippocampal ripples which in turn feed back into ongoing cycles of the thalamo-cortical spindle to effectively modulate the input to neocortical neurons (Mölle et al., 2009; Sirota et al., 2003).

Hippocampo-neocortical connectivity

Further support for a close sleep-dependent coupling between neocortical regions and the hippocampus comes from recent resting-state fMRI work showing increased hippocampo-fusiform functional connectivity during light sleep after face-location learning compared to post-learning wakefulness (van Dongen et al., 2011) and, learning-unrelated, a principal increase in functional connectivity between the hippocampal subiculum and neocortical sites related to the occurrence

of fast sleep spindles (Andrade et al., 2011). Resting-state fMRI studies have also revealed that thalamo-cortical connectivity decreases during the transition from wakefulness to light sleep (Spoormaker et al., 2010) while cortico-cortical connectivity is initially maintained or even increased (Larson-Prior et al., 2009; Spoormaker et al., 2010) before breaking down with the transition to deep slow wave sleep (Spoormaker et al., 2010), in particular within the default mode network (Horovitz et al., 2009; Sämann et al., 2011). The fact that default network connectivity changed continuously with increasing slow wave activity (Horovitz et al., 2009) and hippocampo-neocortical connectivity was modulated by spindle occurrence (Andrade et al., 2011) strongly encourages future research to favor specific neuronal oscillations over sleep stages when defining brain states for functional connectivity analyses.

Spindle amplitude variability

The neurophysiological basis of natural variations in spindle amplitude observable in the human surface EEG remains to be clarified. Amplitude differences between successive spindles may be caused by the output of thalamo-cortical neurons as well as the responsiveness of neocortical neurons to thalamic input. It might reflect the synchrony of neuronal activity as much as the number of participating neurons. In this context, it is interesting that thalamic activity per se was markedly enhanced during spindles, but was only marginally modulated by spindle amplitude. Although the thalamus is the core generator of sleep spindles (Steriade and Timofeev, 2003), thalamo-cortical spindle input can be amplified or suppressed by intracortical circuits (Contreras et al., 1997; Kandel and Buzsaki, 1997). These local cortical mechanisms are a likely substrate contributing to the amplitude modulation of successive spindle events.

Learning-dependent increase in spindle-coupled brain activity

Spindle-related fMRI to show temporally specific memory reactivation

Earlier positron emission tomography (PET) studies have shown increased activity of task-related brain regions during rapid eye movement sleep after procedural learning (Maquet et al., 2000) and during slow wave sleep after navigation learning (Peigneux et al., 2004). However, the limited temporal resolution of PET did not allow us to establish a link between these learning-related reactivations and specific electrophysiological phenomena during sleep. Single-trial EEG-fMRI (Debener et al., 2006) now enabled us to determine the brain regions that covary with the ongoing dynamics of the thalamo-cortical sleep spindle as a function of previous learning experience. The explicit modeling of spindle amplitudes proved highly valuable in explaining trial-by-trial variations in the spindle related BOLD response.

Spatial specificity of spindle-coupled reactivation

The localization of neocortical activations during spindles closely resembled that of the category-specific activations during prior learning. This might reflect spindle-coupled re-activation of those neuronal populations representing the previously acquired learning material. Conversely, the learning-specific increase in spindle-coupled hippocampal activation was located slightly posterior to the hippocampal activation associated with previous memory encoding. This observation ties in with previous fMRI studies indicating a topographical dissociation of hippocampal activations during encoding and retrieval along the anterior-posterior axis, with the former being located primarily in the rostral and the latter in the caudal portions of the hippocampus (Lepage et al., 1998; Spaniol et al., 2009).

Hippocampal increase in spindle-coupling depends on learning performance

The learning-specific increase in coupling between spindle amplitude and hippocampal activation was predicted by previous memory acquisition. The individual learning-specific increase in hippocampal activation (relative to the control night) was greater the higher the average recall performance was during prior learning. Although hippocampal activation was individually adjusted to the corresponding control night, we cannot fully exclude that inter-individual differences in general learning capability contribute to this effect as well (Schabus et al., 2006). One might have expected that learning-specific spindle-related hippocampal activation predicts subsequent overnight memory retention. This, however, was not the case. Several considerations might account for this finding: first, we merely recorded fMRI during early sleep after learning whereas subjects continued sleep and thus hippocampal reactivation afterwards. Therefore all subjects might have been able to sufficiently consolidate the acquired memories, rendering initial hippocampal activation unpredictive for delayed recall one day later. Second, the offline reorganization of hippocampal–neocortical memory traces is not inevitably accompanied by immediate behavioral consequences (Orban et al., 2006). However, the current study was not explicitly designed to detect sleep-dependent changes in recall-related activation. The observed overnight increase in recall-related brain activation was also not predicted by the individual learning-specific increase in hippocampal spindle-coupling and may be attributed to non-sleep effects as well (like the mere recovery from repetition suppression after ~70 min of face/scene processing).

Sleep spindles as a potential mechanism for system memory consolidation

The highly specific increases in spindle-coupled neuronal activity after learning suggest a direct involvement of spindles in the reactivation of previously acquired hippocampal-neocortical memory traces. The increase in spindle-coupled neuronal activity might be caused by an increased responsiveness of hippocampal-neocortical circuitry to thalamo-cortical spindle input after synaptic potentiation (Werk et al., 2005) as well as by increased re-entrant activity from the hippocampal system (Sirota et al., 2003) in terms of sharp wave-ripple activity. It is, however, still possible that the observed spindle-coupled reactivation is a mere epiphenomenon of previously potentiated synaptic connections, and this possibility cannot be ruled out based on neuroimaging data due to its correlative nature. In fact, a demonstration of causality would require an active manipulation of ongoing spindle activity similar to the disruption of hippocampal ripples by electrical stimulation in the rat causing an impairment in spatial memory consolidation (Ego-Stengel and Wilson, 2009; Girardeau et al., 2009). However, as outlined above, spindles are closely linked to hippocampal ripples, and several human studies could indeed demonstrate that learning-related increases in spindle power or density predict overnight changes in memory performance (Clemens et al., 2005, 2006; Schabus et al., 2004, 2008; Schmidt et al., 2006). In our view, spindles are therefore likely to serve an important function in organizing hippocampo-neocortical information flow and gating synaptic plasticity within neocortical circuits.

The question remains why exposure to an experimental learning task is often sufficient to leave a detectable trace in subsequent sleep although subjects during the same night might also reactivate a variety of other memories that had been acquired earlier. In the current study subjects also showed no learning-dependent increase in total spindle number that could reflect some task-related additional reactivation. One possible explanation is that the hippocampus handles memory reactivation in a last-in-first-out manner, ensuring that more recent and thus more labile memory traces are reactivated by earlier spindles, whereas older, more stabilized ones are reactivated later during the night. Alternatively, all memories might be replayed either during the same or during intermingled spindles, with new memories just being reactivated more intensely or more frequently than older ones, respectively. In either case, the proportion of reactivation related to the new memory traces might increase after

learning rather than total spindle number. Future research has to further elucidate the relationship between single spindle events and distinct memory traces.

Learning-specific spindle-related brain activation independent of amplitude

After learning we also found small clusters of increased activity during sleep spindles in left head of the caudate nucleus, amygdala, and brainstem that were not modulated by spindle amplitude (Fig. 4; Supplementary Table S9). Although these activations were not explicitly predicted by our hypothesis and should therefore be interpreted with care, they are plausible in the context of previous work. Though not directly overlapping, adjacent parts of caudate nuclei and amygdalae were also activated during prior learning. The caudate nucleus is involved in stimulus–response learning and interacts with the hippocampal system (Poldrack and Rodriguez, 2004) whereas the amygdala is typically involved in the processing of faces and other social stimuli (Adolphs and Spezio, 2006). Both have previously been shown in the context of sleep-dependent memory consolidation (Orban et al., 2006; Sterpenich et al., 2009). The brainstem cluster might roughly correspond to the locus coeruleus (LC) complex (Keren et al., 2009; Minzenberg et al., 2008; Schmidt et al., 2009). However, LC identification from BOLD fMRI is diversely discussed (Astafiev et al., 2010; Minzenberg et al., 2010; Schmidt et al., 2010) and we cannot reliably identify it from the current data so that this interpretation remains speculative. A learning-related coactivation of the LC during sleep spindles would at least fit into the framework of noradrenergic impact on learning-related plasticity (Sara, 2009) and memory consolidation during sleep (Diekelmann and Born, 2010). Indeed, entrainment of LC bursts to the SO (Lestienne et al., 1997) and increased LC firing during post-leaning SWS have been reported in the rat (Eschenko and Sara, 2008). Increased LC activity during spindles after learning may thus set the neuromodulatory stage for synaptic potentiation, making spindles effective windows of cortical plasticity during NonREM sleep (Sejnowski and Destexhe, 2000; Steriade and Timofeev, 2003).

Conclusion

Our results extend existing knowledge in two important aspects: first, the reactivation of stimulus category-specific brain regions is time-locked to individual sleep spindles and tightly coupled to spindle amplitude, rather than being evenly distributed throughout NonREM sleep. Second, spindle-coupled reactivation is topographically specific to the neocortical representations that might have been associated by the hippocampus during prior learning. Together, our results suggest an important role of sleep spindles in the reactivation and resultant redistribution of hippocampal–neocortical memory traces during sleep.

Acknowledgments

This work was supported by the Deutsche Forschungsgemeinschaft (Project A6, SFB 654 'Plasticity and Sleep') and the Bundesministerium für Bildung und Forschung (01GO0511 'NeuroImageNord' to H.R.S.). H.R.S. was further supported by a Grant of Excellence "ContAct" from Lundbeckfonden (R59 A5399). We thank Olav Jansen for providing the MRI infrastructure, Kristoffer H. Madsen for help with cardiac noise modeling and explicit filter functions, Oliver Granert for computational assistance, and Björn Rasch for helpful comments on an earlier version of this manuscript.

Appendix A. Supplementary data

Supplementary data to this article can be found online at doi:10.1016/j.neuroimage.2011.10.036.

References

Achermann, P., Borbely, A.A., 1997. Low-frequency (< 1 Hz) oscillations in the human sleep electroencephalogram. Neuroscience 81, 213–222.
Adolphs, R., Spezio, M., 2006. Role of the amygdala in processing visual social stimuli. Prog. Brain Res. 156, 363–378.
Allen, P.J., Polizzi, G., Krakow, K., Fish, D.R., Lemieux, L., 1998. Identification of EEG events in the MR scanner: the problem of pulse artifact and a method for its subtraction. Neuroimage 8, 229–239.
Allen, P.J., Josephs, O., Turner, R., 2000. A method for removing imaging artifact from continuous EEG recorded during functional MRI. Neuroimage 12, 230–239.
Andrade, K.C., Spoormaker, V.I., Dresler, M., Wehrle, R., Holsboer, F., Samann, P.G., Czisch, M., 2011. Sleep spindles and hippocampal functional connectivity in human NREM sleep. J. Neurosci. 31, 10331–10339.
Astafiev, S.V., Snyder, A.Z., Shulman, G.L., Corbetta, M., 2010. Comment on "modafinil shifts human locus coeruleus to low-tonic, high-phasic activity during functional MRI" and "homeostatic sleep pressure and responses to sustained attention in the suprachiasmatic area". Science 328, 309 (author reply 309).
Buzsaki, G., 1996. The hippocampo-neocortical dialogue. Cereb. Cortex 6, 81–92.
Clemens, Z., Fabo, D., Halasz, P., 2005. Overnight verbal memory retention correlates with the number of sleep spindles. Neuroscience 132, 529–535.
Clemens, Z., Fabo, D., Halasz, P., 2006. Twenty-four hours retention of visuospatial memory correlates with the number of parietal sleep spindles. Neurosci. Lett. 403, 52–56.
Clemens, Z., Mölle, M., Eross, L., Barsi, P., Halasz, P., Born, J., 2007. Temporal coupling of parahippocampal ripples, sleep spindles and slow oscillations in humans. Brain 130, 2868–2878.
Clemens, Z., Mölle, M., Eross, L., Jakus, R., Rasonyi, G., Halasz, P., Born, J., 2010. Fine-tuned coupling between human parahippocampal ripples and sleep spindles. Eur. J. Neurosci. 33, 511–520.
Contreras, D., Destexhe, A., Steriade, M., 1997. Intracellular and computational characterization of the intracortical inhibitory control of synchronized thalamic inputs in vivo. J. Neurophysiol. 78, 335–350.
Dang-Vu, T.T., Schabus, M., Desseilles, M., Albouy, G., Boly, M., Darsaud, A., Gais, S., Rauchs, G., Sterpenich, V., Vandewalle, G., Carrier, J., Moonen, G., Balteau, E., Degueldre, C., Luxen, A., Phillips, C., Maquet, P., 2008. Spontaneous neural activity during human slow wave sleep. Proc. Natl. Acad. Sci. U.S.A. 105, 15160–15165.
Debener, S., Ullsperger, M., Siegel, M., Engel, A.K., 2006. Single-trial EEG-fMRI reveals the dynamics of cognitive function. Trends Cogn. Sci. 10, 558–563.
Diekelmann, S., Born, J., 2010. The memory function of sleep. Nat. Rev. Neurosci. 11, 114–126.
Ego-Stengel, V., Wilson, M.A., 2009. Disruption of ripple-associated hippocampal activity during rest impairs spatial learning in the rat. Hippocampus 20, 1–10.
Eichenbaum, H., 2000. A cortical–hippocampal system for declarative memory. Nat. Rev. Neurosci. 1, 41–50.
Epstein, R., Kanwisher, N., 1998. A cortical representation of the local visual environment. Nature 392, 598–601.
Eschenko, O., Sara, S.J., 2008. Learning-dependent, transient increase of activity in noradrenergic neurons of locus coeruleus during slow wave sleep in the rat: brain stem-cortex interplay for memory consolidation? Cereb. Cortex 18, 2596–2603.
Eschenko, O., Mölle, M., Born, J., Sara, S.J., 2006. Elevated sleep spindle density after learning or after retrieval in rats. J. Neurosci. 26, 12914–12920.
Fogel, S.M., Smith, C.T., 2006. Learning-dependent changes in sleep spindles and Stage 2 sleep. J. Sleep Res. 15, 250–255.
Frankland, P.W., Bontempi, B., 2005. The organization of recent and remote memories. Nat. Rev. Neurosci. 6, 119–130.
Gais, S., Mölle, M., Helms, K., Born, J., 2002. Learning-dependent increases in sleep spindle density. J. Neurosci. 22, 6830–6834.
Gauthier, I., Tarr, M.J., Moylan, J., Skudlarski, P., Gore, J.C., Anderson, A.W., 2000. The fusiform "face area" is part of a network that processes faces at the individual level. J. Cogn. Neurosci. 12, 495–504.
Girardeau, G., Benchenane, K., Wiener, S.I., Buzsaki, G., Zugaro, M.B., 2009. Selective suppression of hippocampal ripples impairs spatial memory. Nat. Neurosci. 12, 1222–1223.
Glover, G.H., Li, T.Q., Ress, D., 2000. Image-based method for retrospective correction of physiological motion effects in fMRI: RETROICOR. Magn. Reson. Med. 44, 162–167.
Hoddes, E., Zarcone, V., Smythe, H., Phillips, R., Dement, W.C., 1973. Quantification of sleepiness: a new approach. Psychophysiology 10, 431–436.
Horovitz, S.G., Braun, A.R., Carr, W.S., Picchioni, D., Balkin, T.J., Fukunaga, M., Duyn, J.H., 2009. Decoupling of the brain's default mode network during deep sleep. Proc. Natl. Acad. Sci. U.S.A. 106, 11376–11381.
Johnson, L.A., Euston, D.R., Tatsuno, M., McNaughton, B.L., 2010. Stored-trace reactivation in rat prefrontal cortex is correlated with down-to-up state fluctuation density. J. Neurosci. 30, 2650–2661.
Kandel, A., Buzsaki, G., 1997. Cellular-synaptic generation of sleep spindles, spike-and-wave discharges, and evoked thalamocortical responses in the neocortex of the rat. J. Neurosci. 17, 6783–6797.
Kanwisher, N., McDermott, J., Chun, M.M., 1997. The fusiform face area: a module in human extrastriate cortex specialized for face perception. J. Neurosci. 17, 4302–4311.
Keren, N.I., Lozar, C.T., Harris, K.C., Morgan, P.S., Eckert, M.A., 2009. In vivo mapping of the human locus coeruleus. Neuroimage 47, 1261–1267.
Larson-Prior, L.J., Zempel, J.M., Nolan, T.S., Prior, F.W., Snyder, A.Z., Raichle, M.E., 2009. Cortical network functional connectivity in the descent to sleep. Proc. Natl. Acad. Sci. U.S.A. 106, 4489–4494.
Lepage, M., Habib, R., Tulving, E., 1998. Hippocampal PET activations of memory encoding and retrieval: the HIPER model. Hippocampus 8, 313–322.

Lestienne, R., Herve-Minvielle, A., Robinson, D., Briois, L., Sara, S.J., 1997. Slow oscillations as a probe of the dynamics of the locus coeruleus-frontal cortex interaction in anesthetized rats. J. Physiol. Paris 91, 273–284.
Maquet, P., 2001. The role of sleep in learning and memory. Science 294, 1048–1052.
Maquet, P., Laureys, S., Peigneux, P., Fuchs, S., Petiau, C., Phillips, C., Aerts, J., Del Fiore, G., Degueldre, C., Meulemans, T., Luxen, A., Franck, G., Van Der Linden, M., Smith, C., Cleeremans, A., 2000. Experience-dependent changes in cerebral activation during human REM sleep. Nat. Neurosci. 3, 831–836.
Marshall, L., Born, J., 2007. The contribution of sleep to hippocampus-dependent memory consolidation. Trends Cogn. Sci. 11, 442–450.
McClelland, J.L., McNaughton, B.L., O'Reilly, R.C., 1995. Why there are complementary learning systems in the hippocampus and neocortex: insights from the successes and failures of connectionist models of learning and memory. Psychol. Rev. 102, 419–457.
Minzenberg, M.J., Watrous, A.J., Yoon, J.H., Ursu, S., Carter, C.S., 2008. Modafinil shifts human locus coeruleus to low-tonic, high-phasic activity during functional MRI. Science 322, 1700–1702.
Minzenberg, M.J., Watrous, A.J., Yoon, J.H., La, C., Ursu, S., Carter, C.S., 2010. Response to comment on "modafinil shifts human locus coeruleus to low-tonic, high-phasic activity during functional MRI". Science 328, 309.
Mölle, M., Born, J., 2009. Hippocampus whispering in deep sleep to prefrontal cortex — for good memories? Neuron 61, 496–498.
Mölle, M., Marshall, L., Gais, S., Born, J., 2002. Grouping of spindle activity during slow oscillations in human non-rapid eye movement sleep. J. Neurosci. 22, 10941–10947.
Mölle, M., Yeshenko, O., Marshall, L., Sara, S.J., Born, J., 2006. Hippocampal sharp wave-ripples linked to slow oscillations in rat slow-wave sleep. J. Neurophysiol. 96, 62–70.
Mölle, M., Eschenko, O., Gais, S., Sara, S.J., Born, J., 2009. The influence of learning on sleep slow oscillations and associated spindles and ripples in humans and rats. Eur. J. Neurosci. 29, 1071–1081.
Orban, P., Rauchs, G., Balteau, E., Degueldre, C., Luxen, A., Maquet, P., Peigneux, P., 2006. Sleep after spatial learning promotes covert reorganization of brain activity. Proc. Natl. Acad. Sci. U.S.A. 103, 7124–7129.
Peigneux, P., Laureys, S., Fuchs, S., Collette, F., Perrin, F., Reggers, J., Phillips, C., Degueldre, C., Del Fiore, G., Aerts, J., Luxen, A., Maquet, P., 2004. Are spatial memories strengthened in the human hippocampus during slow wave sleep? Neuron 44, 535–545.
Peyrache, A., Khamassi, M., Benchenane, K., Wiener, S.I., Battaglia, F.P., 2009. Replay of rule-learning related neural patterns in the prefrontal cortex during sleep. Nat. Neurosci. 12, 919–926.
Poldrack, R.A., Mumford, J.A., 2009. Independence in ROI analysis: where is the voodoo? Soc. Cogn. Affect. Neurosci. 4, 208–213.
Poldrack, R.A., Rodriguez, P., 2004. How do memory systems interact? Evidence from human classification learning. Neurobiol. Learn. Mem. 82, 324–332.
Rasch, B., Born, J., 2007. Maintaining memories by reactivation. Curr. Opin. Neurobiol. 17, 698–703.
Rechtschaffen, A., Kales, A., 1968. A Manual of Standardized Terminology, Techniques and Scoring System for Sleep Stages of Human Subjects. United States Government Printing Office, Washington, DC.
Sämann, P.G., Wehrle, R., Hoehn, D., Spoormaker, V.I., Peters, H., Tully, C., Holsboer, F., Czisch, M., 2011. Development of the Brain's default mode network from wakefulness to slow wave sleep. Cereb. Cortex 21, 2082–2093.
Sara, S.J., 2009. The locus coeruleus and noradrenergic modulation of cognition. Nat. Rev. Neurosci. 10, 211–223.
Schabus, M., Gruber, G., Parapatics, S., Sauter, C., Klosch, G., Anderer, P., Klimesch, W., Saletu, B., Zeitlhofer, J., 2004. Sleep spindles and their significance for declarative memory consolidation. Sleep 27, 1479–1485.
Schabus, M., Hodlmoser, K., Gruber, G., Sauter, C., Anderer, P., Klosch, G., Parapatics, S., Saletu, B., Klimesch, W., Zeitlhofer, J., 2006. Sleep spindle-related activity in the human EEG and its relation to general cognitive and learning abilities. Eur. J. Neurosci. 23, 1738–1746.
Schabus, M., Dang-Vu, T.T., Albouy, G., Balteau, E., Boly, M., Carrier, J., Darsaud, A., Degueldre, C., Desseilles, M., Gais, S., Phillips, C., Rauchs, G., Schnakers, C., Sterpenich, V., Vandewalle, G., Luxen, A., Maquet, P., 2007. Hemodynamic cerebral correlates of sleep spindles during human non-rapid eye movement sleep. Proc. Natl. Acad. Sci. U.S.A. 104, 13164–13169.
Schabus, M., Hoedlmoser, K., Pecherstorfer, T., Anderer, P., Gruber, G., Parapatics, S., Sauter, C., Kloesch, G., Klimesch, W., Saletu, B., Zeitlhofer, J., 2008. Interindividual sleep spindle differences and their relation to learning-related enhancements. Brain Res. 1191, 127–135.
Schmidt, C., Peigneux, P., Muto, V., Schenkel, M., Knoblauch, V., Munch, M., de Quervain, D.J., Wirz-Justice, A., Cajochen, C., 2006. Encoding difficulty promotes postlearning changes in sleep spindle activity during napping. J. Neurosci. 26, 8976–8982.
Schmidt, C., Collette, F., Leclercq, Y., Sterpenich, V., Vandewalle, G., Berthomier, P., Berthomier, C., Phillips, C., Tinguely, G., Darsaud, A., Gais, S., Schabus, M., Desseilles, M., Dang-Vu, T.T., Salmon, E., Balteau, E., Degueldre, C., Luxen, A., Maquet, P., Cajochen, C., Peigneux, P., 2009. Homeostatic sleep pressure and responses to sustained attention in the suprachiasmatic area. Science 324, 516–519.
Schmidt, C., Peigneux, P., Maquet, P., Phillips, C., 2010. Response to comment on "homeostatic sleep pressure and responses to sustained attention in the suprachiasmatic area". Science 328, 309.
Sejnowski, T.J., Destexhe, A., 2000. Why do we sleep? Brain Res. 886, 208–223.
Siapas, A.G., Wilson, M.A., 1998. Coordinated interactions between hippocampal ripples and cortical spindles during slow-wave sleep. Neuron 21, 1123–1128.
Sirota, A., Csicsvari, J., Buhl, D., Buzsaki, G., 2003. Communication between neocortex and hippocampus during sleep in rodents. Proc. Natl. Acad. Sci. U.S.A. 100, 2065–2069.
Spaniol, J., Davidson, P.S., Kim, A.S., Han, H., Moscovitch, M., Grady, C.L., 2009. Event-related fMRI studies of episodic encoding and retrieval: meta-analyses using activation likelihood estimation. Neuropsychologia 47, 1765–1779.
Spoormaker, V.I., Schroter, M.S., Gleiser, P.M., Andrade, K.C., Dresler, M., Wehrle, R., Samann, P.G., Czisch, M., 2010. Development of a large-scale functional brain network during human non-rapid eye movement sleep. J. Neurosci. 30, 11379–11387.
Steriade, M., 2006. Grouping of brain rhythms in corticothalamic systems. Neuroscience 137, 1087–1106.
Steriade, M., Timofeev, I., 2003. Neuronal plasticity in thalamocortical networks during sleep and waking oscillations. Neuron 37, 563–576.
Steriade, M., Nunez, A., Amzica, F., 1993. A novel slow (<1 Hz) oscillation of neocortical neurons in vivo: depolarizing and hyperpolarizing components. J. Neurosci. 13, 3252–3265.
Sterpenich, V., Albouy, G., Darsaud, A., Schmidt, C., Vandewalle, G., Dang Vu, T.T., Desseilles, M., Phillips, C., Degueldre, C., Balteau, E., Collette, F., Luxen, A., Maquet, P., 2009. Sleep promotes the neural reorganization of remote emotional memory. J. Neurosci. 29, 5143–5152.
Stickgold, R., 2005. Sleep-dependent memory consolidation. Nature 437, 1272–1278.
Sutherland, G.R., McNaughton, B., 2000. Memory trace reactivation in hippocampal and neocortical neuronal ensembles. Curr. Opin. Neurobiol. 10, 180–186.
Van Der Werf, Y.D., Altena, E., Schoonheim, M.M., Sanz-Arigita, E.J., Vis, J.C., De Rijke, W., Van Someren, E.J., 2009. Sleep benefits subsequent hippocampal functioning. Nat. Neurosci. 12, 122–123.
van Dongen, E.V., Takashima, A., Barth, M., Fernandez, G., 2011. Functional connectivity during light sleep is correlated with memory performance for face-location associations. Neuroimage 57, 262–270.
Werk, C.M., Harbour, V.L., Chapman, C.A., 2005. Induction of long-term potentiation leads to increased reliability of evoked neocortical spindles in vivo. Neuroscience 131, 793–800.
Wierzynski, C.M., Lubenov, E.V., Gu, M., Siapas, A.G., 2009. State-dependent spike-timing relationships between hippocampal and prefrontal circuits during sleep. Neuron 61, 587–596.
Yoo, S.S., Hu, P.T., Gujar, N., Jolesz, F.A., Walker, M.P., 2007. A deficit in the ability to form new human memories without sleep. Nat. Neurosci. 10, 385–392.